J Comput Aided Mol Des (2008) 22:661–671
DOI 10.1007/s10822-007-9144-9

Rational design of an enzyme mutant for anti-cocaine therapeutics

Fang Zheng · Chang-Guo Zhan

Received: 20 August 2007 / Accepted: 24 October 2007 / Published online: 8 November 2007
© Springer Science+Business Media B.V. 2007

Abstract (−)-Cocaine is a widely abused drug and there is no available anti-cocaine therapeutic. The disastrous medical and social consequences of cocaine addiction have made the development of an effective pharmacological treatment a high priority. An ideal anti-cocaine medication would be to accelerate (−)-cocaine metabolism producing biologically inactive metabolites. The main metabolic pathway of cocaine in body is the hydrolysis at its benzoyl ester group. Reviewed in this article is the state-of-the-art computational design of high-activity mutants of human butyrylcholinesterase (BChE) against (−)-cocaine. The computational design of BChE mutants have been based on not only the structure of the enzyme, but also the detailed catalytic mechanisms for BChE-catalyzed hydrolysis of (−)-cocaine and (+)-cocaine. Computational studies of the detailed catalytic mechanisms and the structure-and-mechanism-based computational design have been carried out through the combined use of a variety of state-of-the-art techniques of molecular modeling. By using the computational insights into the catalytic mechanisms, a recently developed unique computational design strategy based on the simulation of the rate-determining transition state has been employed to design high-activity mutants of human BChE for hydrolysis of (−)-cocaine, leading to the exciting discovery of BChE mutants with a considerably improved catalytic efficiency against (−)-cocaine. One of the discovered BChE mutants (i.e., A199S/S287G/A328W/Y332G) has a ~456-fold improved catalytic efficiency against (−)-cocaine. The encouraging outcome of the computational design and discovery effort demonstrates that the unique computational design approach based on the transition-state simulation is promising for rational enzyme redesign and drug discovery.

Keywords Cocaine abuse · Anti-cocaine medication · Hydrolysis mechanism · Transition state · Enzymatic reaction · Rational enzyme redesign

F. Zheng · C.-G. Zhan (✉)
Department of Pharmaceutical Sciences, College of Pharmacy, University of Kentucky, 725 Rose Street, Lexington, KY 40536, USA
e-mail: zhan@uky.edu

Introduction

Cocaine abuse is a major medical and public health problem that continues to defy treatment [1–4]. The disastrous medical and social consequences of cocaine addiction, such as violent crime, loss in individual productivity, illness and death, have made the development of an effective pharmacological treatment a high priority [5, 6]. Most of previously employed anti-addiction strategies use the classical pharmacodynamic approach, i.e., developing small molecules that interact with one or more neuronal binding sites, with the goal of blocking or counteracting a drug's neuropharmacological actions. However, despite decades of effort, existing pharmacodynamic approaches to cocaine abuse treatment have not yet proven successful [5–8]. The inherent difficulties in antagonizing a blocker-like cocaine have led to the development of the pharmacokinetic approach that aims at acting directly on the drug itself to alter its distribution or accelerate its clearance [7–14].

Pharmacokinetic antagonism of cocaine could be implemented by administration of a molecule, such as an anti-cocaine antibody, which binds tightly to cocaine so as to prevent cocaine from crossing the blood-brain barrier [15–21]. The blocking action could also be implemented

by administration of an enzyme or a catalytic antibody (regarded as an artificial enzyme) that not only binds but also accelerates cocaine metabolism and thereby freeing itself for further binding [16–26]. Usually, a pharmacokinetic agent would not be expected to cross the blood-brain barrier and thus would itself have no direct pharmacodynamic action, such as abuse liability [5].

An ideal pharmacokinetic agent for this purpose should be a potent enzyme catalyzing the hydrolysis of cocaine into biologically inactive metabolites. The dominant pathway for cocaine metabolism in primates is butyrylcholinesterase (BChE)-catalyzed hydrolysis at the benzoyl ester group (Fig. 1) and the metabolites are all biologically inactive [5, 6]. Clearly, BChE-catalyzed hydrolysis of cocaine at the benzoyl ester is the metabolic pathway most suitable for amplification. However, the catalytic activity of this plasma enzyme is about a 1000-fold lower against the naturally occurring (−)-cocaine than that against the biologically inactive (+)-cocaine enantiomer [27–30]. (+)-cocaine can be cleared from plasma in seconds and prior to partitioning into the central nervous system (CNS), whereas (−)-cocaine has a plasma half-life of ∼45–90 min, long enough for manifestation of the CNS effects which peak in minutes [5]. Hence, BChE mutants with a higher activity against (−)-cocaine are highly desirable for use as an exogenous enzyme in humans. We note that the native human BChE itself has been used as an exogenous enzyme in clinic for other purposes [5]. Other currently used exogenous enzymes as therapeutics include agalsidase beta (Fabrazyme (R)) which is a recombinant human alpha-galactosidase A enzyme approved for intravenous use in the treatment of Fabry disease [31].

Generally speaking, for rational design of a mutant enzyme with a higher catalytic activity for a given substrate, one needs to design a mutation that can accelerate the rate-determining step of the entire catalytic reaction process while the other steps are not slowed down by the mutation. Hence, in order to rationally design high-activity mutants of human BChE, one first needs to understand the fundamental mechanisms for BChE-catalyzed hydrolysis of (−)-cocaine and (+)-cocaine. As discussed below, encouraging progress has been made in understanding the catalytic mechanisms and computational design of high-activity mutants of human BChE. Below, we will first discuss the catalytic mechanisms and then discuss the structure-and-mechanism-based design of the high-activity mutants of human BChE.

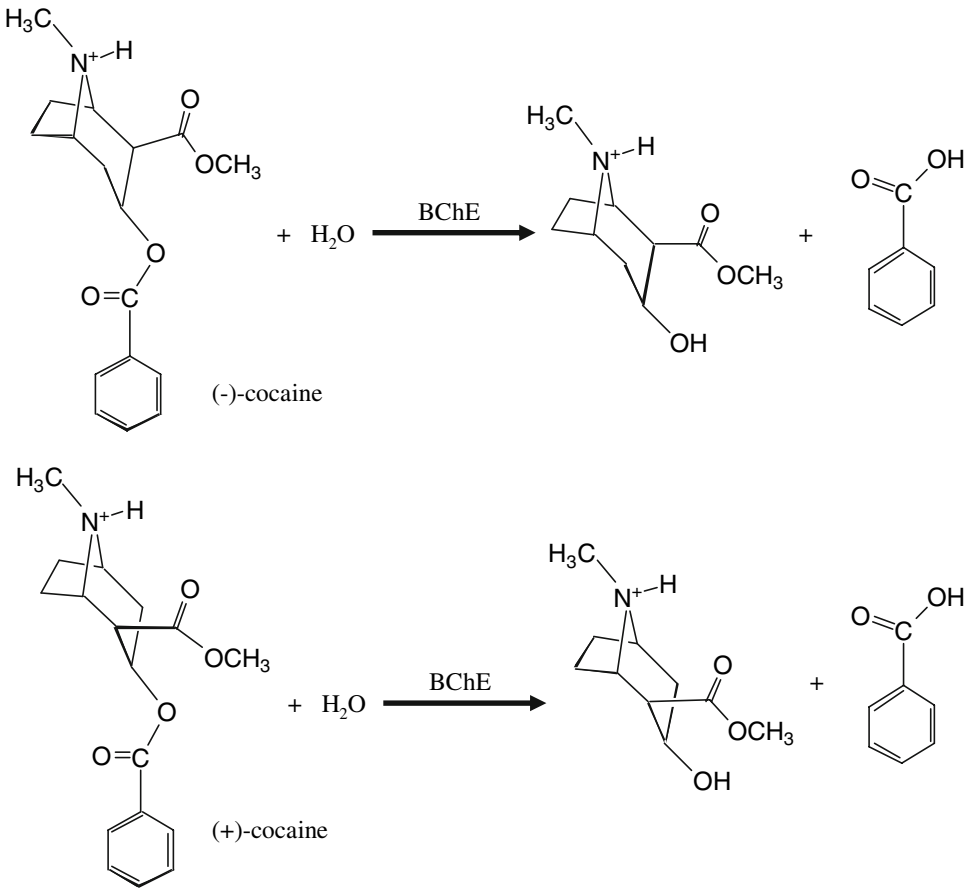

Fig. 1 Hydrolysis of (−)-cocaine and (+)-cocaine

Catalytic mechanism for BChE-catalyzed hydrolysis of cocaine

BChE binding with its substrates

Reaction coordinate calculations for an enzymatic reaction begin with a concept of the enzyme–substrate binding in the prereactive enzyme–substrate complex. Different starting structures for the enzyme–substrate complex can lead to completely different reactions. The initial insights into the enzyme–substrate binding came from a comparison of the optimized geometry of butyrylcholine (BCh) with those of (−)-cocaine and (+)-cocaine [32].

In human BChE, W82 is thought to be the key factor in the stabilization of positively charged substrates in the BChE-substrate complexes, although this interaction should be more properly classified as a cation-π interaction [33]. While the positively charged quaternary ammonium is positioned to effectively bind with W82 in the prereactive BChE-substrate complex, the carbonyl carbon of the substrate must be positioned proximal to S198 O^{γ} for nucleophilic attack. Thus the distance between the carbonyl carbon and the quaternary ammonium is critical and, according to the optimized geometries [32], this distance is 4.92 Å for the excellent substrate BCh. The optimized C–N distance for the substrate cocaine benzoyl ester (5.23 Å) is similar to that of BCh. The C–N distance for the cocaine methyl ester (2.95 Å) is remarkably shorter. This helps to explain why (−)-cocaine and (+)-cocaine bind with BChE in a way to hydrolyze at the benzoyl ester, instead of the methyl ester, whereas for the non-enzymatic hydrolysis of cocaine under physiological conditions (pH 7.4; 37°) the methyl ester hydrolyzes faster than the benzoyl [34, 35].

Based on the structural similarity discussed above and further molecular dynamics (MD) simulations [32], the relative positions of the positively charged quaternary ammonium and the carbonyl group of the benzoyl ester moiety in the prereactive BChE–cocaine complexes are similar to that in the corresponding BChE-BCh complex. The main structural difference between the BChE–(−)-cocaine and BChE–(+)-cocaine complexes exists only in the relative position of the methyl ester group. The MD trajectories [32] reveal that in both the BChE–(−)-cocaine and BChE–(+)-cocaine complexes, the cocaine nitrogen atom stays at nearly the same position as the BCh nitrogen atom in the structure of BChE model constructed by Harel et al. [36]. The computational results suggest that both (−)-cocaine and (+)-cocaine may bind with human BChE so as to allow S198 O^{γ} to approach the carbonyl carbon of the benzoyl ester. The simulated structures of the prereactive BChE–(−)-cocaine and BChE–(+)-cocaine complexes are similar to the prereactive enzyme–substrate structure proposed for Chew binding with other positively charged substrates, i.e., butyrylthiocholine and succinyldithiocholine [33, 37]; they are all positioned horizontally at the bottom of the substrate-binding gorge of BChE.

To better understand BChE binding with cocaine, (−)-cocaine and (+)-cocaine were also docked to the BChE active site in order to model the non-prereactive enzyme–substrate complexes [32]. In the MD-simulated non-prereactive BChE–(−)-cocaine and BChE–(+)-cocaine complexes, (−)-cocaine and (+)-cocaine are positioned vertically in the substrate-binding gorge between D70 and W82. The MD trajectories for the non-prereactive BChE–(−)-cocaine and BChE–(+)-cocaine complexes are also very stable. In addition, the simulated non-prereactive BChE–(−)-cocaine and BChE–(+)-cocaine complexes are very close to the simulated Michaelis–Menten complexes reported by Sun et al. [38]. All these suggest that the binding of BChE with (−)-cocaine and (+)-cocaine is similar to those proposed with butyrylthiocholine and succinyldithiocholine. Both the non-prereactive and prereactive enzyme–substrate complexes could exist before going to the chemical reaction steps [32].

For further comparison between the modeled non-prereactive complex and the prereactive complex for BChE binding (−)-cocaine and (+)-cocaine, the protein backbone atoms in the non-prereactive complex were superimposed with the corresponding atoms in the prereactive complex [32]. It turns out that the overall protein structures in the non-prereactive and prereactive complexes are very close to each other, while the orientations of the substrate are nearly vertical to each other. So, for both (−)-cocaine and (+)-cocaine, the substrate needs to rotate about 90° [32] during the change from the non-prereactive complex to the prereactive complex; more specifically, (−)-cocaine needs to rotate slightly more than (+)-cocaine. Depicted in Fig. 2 are the simulated structures of the non-prereactive and prereactive BChE–(−)-cocaine complexes. The cocaine rotation has been discussed in literature in detail based on the MD simulations on both the non-prereactive and prereactive complexes [32, 46]. The energy barrier of the change from the non-prereactive complex to the prereactive complex for (−)-cocaine is expected to differ from that for (+)-cocaine. This is because the relative positions of the C-2 methyl ester group of substrate are different and, therefore, some amino acid residues hindering the rotation of one substrate might not hinder the rotation of another. Specific residues possibly hindering (−)-cocaine rotation will be discussed below.

Fundamental reaction pathway for BChE-catalyzed hydrolysis of (−)-cocaine and (+)-cocaine

For both (−)-cocaine and (+)-cocaine, the relative positions of the nitrogen and the benzoyl carbonyl in the simulated

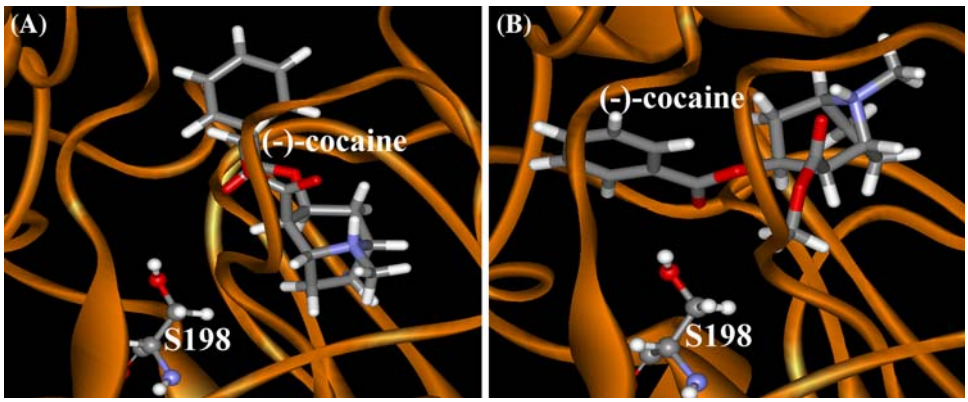

Fig. 2 BChE binding site in the simulated non-prereactive complex of (−)-cocaine with wild-type BChE (**a**) and the prereactive complex of (−)-cocaine with wild-type BChE (**b**) [46]

prereactive BChE-substrate complex are essentially the same as those reported for BCh in BChE [32], one may expect that BChE-catalyzed hydrolysis of (−)-cocaine and (+)-cocaine follow a reaction pathway similar to that for BChE-catalyzed hydrolysis of BCh. A remarkable difference between (−)-cocaine and (+)-cocaine is associated with the relative position of the C-2 methyl ester group. The C-2 methyl ester group of (−)-cocaine remains on the same side of the carbonyl of the benzoyl ester as the attacking hydroxyl oxygen (S198 O^{γ}), whereas the C-2 methyl ester of (+)-cocaine remains on the opposite side. This difference could cause a difference in hydrogen bonding, electrostatic, and van der Waals interactions during the catalytic process, and result in a significant difference in free energies of activation. Nevertheless, the basic BChE mechanism for both enantiomers may resemble the common catalytic mechanism for ester hydrolysis in other serine hydrolases [32, 39], including the thoroughly investigated AChE [40–44].

The molecular docking and MD simulations [32] demonstrate that (−)-cocaine/(+)-cocaine first slides down the substrate-binding gorge to bind to W82 and stands vertically in the gorge between D70 and W82 (non-prereactive complex) and then rotates to a position in the catalytic site within a favorable distance for nucleophilic attack and hydrolysis by S198 (prereactive complex). In the prereactive complex, cocaine lies horizontally at the bottom of the gorge. The main structural difference between the BChE-(−)-cocaine complexes and the corresponding BChE-(+)-cocaine complexes is in the relative position of the cocaine methyl ester group.

Further, starting from the prereactive complexes and the knowledge about ester hydrolysis in other serine hydrolases, a possible chemical reaction pathway for BChE-catalyzed hydrolysis of cocaine was hypothesized [32]. Fig. 3 depicts (−)-cocaine and important groups from the catalytic triad (S198, E325, and H438) and three-pronged oxyanion hole (G116, G117, and A199). The BChE-catalyzed hydrolysis of (−)/(+)-cocaine consists of both the acylation and deacylation stages demonstrated for ester hydrolysis by other serine hydrolases. A significant difference might exist in the number of potential hydrogen bonds involving the carbonyl oxygen in the oxyanion hole. The three-pronged oxyanion hole formed by peptidic NH groups of G116, G117, and A199 in BChE (or by peptidic NH groups of G118, G119, and A201 in AChE) contrasts with the two-pronged oxyanion hole of many other serine hydrolases. Schematic representation of the pathway for (+)-cocaine hydrolysis should be similar to Fig. 3, differing only in the relative position of the C-2 methyl ester group in the acylation.

The detailed reaction coordinate calculations [32] confirmed the mechanistic hypothesis depicted in Fig. 3, i.e., the entire chemical reaction process consists of four individual steps (ES → TS1 → INT1 → TS2 → INT2 → TS3 → INT3 → TS4 → EB). As depicted in Fig. 3 [32, 45], the acylation is initialized by S198 O^{γ} attack at the carbonyl carbon of the cocaine benzoyl ester to form the first tetrahedral intermediate (INT1) through the first transition state (TS1). During the formation of INT1, the C–O bond between the carbonyl carbon and S198 O^{γ} gradually forms, while the proton at S198 O^{γ} gradually transfers to the imidazole N atom of H438 which acts as a general base. The second step of the acylation is the decomposition of INT1 to the metabolite ecgonine methyl ester and acyl-BChE (INT2a) through the second transition state (TS2). During the change from INT1 to INT2a, the proton gradually transfers to the benzoyl ester oxygen, while the C–O bond between the carbonyl carbon and the ester oxygen gradually breaks.

All of the computational results [32, 46] in comparison with available experimental data demonstrate the rate-determining step of the BChE-catalyzed hydrolysis of (+)-cocaine is the first step of deacylation, whereas for (−)-cocaine the change from the non-prereactive complex to the prereactive complex is rate determining and has a Gibbs free energy barrier higher than that for the first step of deacylation by $\sim$4 kcal/mol.

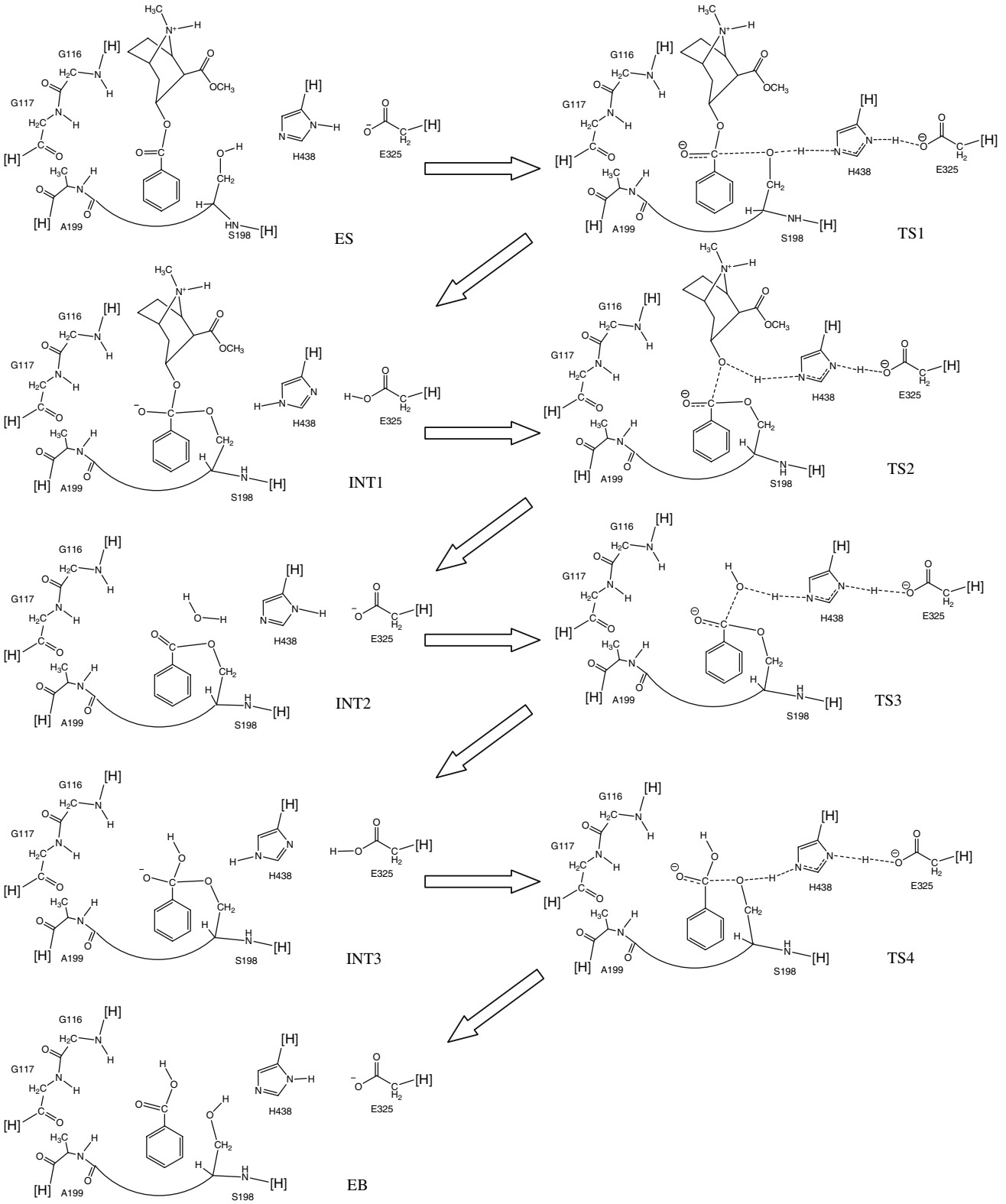

Fig. 3 Schematic representation of BChE-catalyzed hydrolysis of (−)-cocaine. Only QM-treated high-layer part of the reaction system in the ONIOM (QM/MM) calculations [45] are drawn. Notation [H] refers to a non-hydrogen atom in the MM-treated low-layer part of the protein and the cut covalent bond with this atom is saturated by a hydrogen atom. The transition covalent bonds existing in all of the transition states are indicated with dash lines

Design of BChE mutants based on the modeling and simulation of the enzyme-substrate binding

The enzyme–substrate binding and fundamental reaction pathways discussed above provide a rational base for the design of more active BChE mutants for catalytic hydrolysis of (−)-cocaine. Now that the change from the non-prereactive complex to the prereactive complex is the rate-determining step of (−)-cocaine hydrolysis catalyzed by wild-type BChE, useful BChE mutants could be designed to specifically accelerate the change from the non-prereactive BChE–(−)-cocaine complex to the prereactive BChE–(−)-cocaine complex. A detailed analysis [32, 46] of the MD-simulated structures of wild-type BChE binding with (−)-cocaine and (+)-cocaine revealed that Y332 is a key residue hindering the structural change from the non-prereactive BChE–(−)-cocaine complex to the prereactive BChE–(−)-cocaine complex [32, 46]. A number of possible mutants of BChE were proposed for wet experimental tests [32, 38, 46–50]. The earliest design of BChE mutants was only based on the modeled or simulated structure of the non-prereactive BChE–(−)-cocaine complex with wild-type BChE; the possible dynamics of the proposed BChE mutants were not examined. Some of the proposed mutants indeed have a significantly improved catalytic efficiency against (−)-cocaine [32, 38, 46–50].

In order to more reliably predict the BChE mutants with a possibly higher catalytic efficiency against (−)-cocaine, MD simulations were also performed on the structures of (−)-cocaine binding with a number of hypothetical BChE mutants in their non-prereactive and prereactive complexes [46]. Summarized in Table 1 are the average values of some important geometric parameters in the simulated complexes.

In the simulated non-prereactive complex, the average distance between the carbonyl carbon of cocaine benzoyl ester and S198 O^{γ} is 7.6 Å for A328W/Y332A BChE and 7.1 Å for A328W/Y332G BChE, as seen in Table 1. In the simulated prereactive complex, the average values of this important internuclear distance become 3.87 and 3.96 Å for A328W/Y332A and A328W/Y332G BChE's, respectively. Compared to the simulated wild-type BChE–(−)-cocaine prereactive complex, the average distances between the carbonyl carbon of the cocaine benzoyl ester and S198 O^{γ} in the prereactive complex of (−)-cocaine with A328W/Y332A and A328W/Y332G BChE's are all slightly longer, whereas the average distances between the carbonyl oxygen of the cocaine benzoyl ester and the NH of G116, G117, and A199 residues are all shorter. This suggests that (−)-cocaine more strongly binds with A328W/Y332A and A328W/Y332G BChE's in the prereactive complexes. More importantly, the (−)-cocaine rotation in the active site of A328W/Y332A and A328W/Y332G BChE's from the non-prereactive complex to the prereactive complex did not cause considerable changes of the positions of A332 (or G332), W328, and F329 residues, compared to the (−)-cocaine rotation in the active site of wild-type BChE. These results suggest that A328W/Y332A and A328W/Y332G BChE's should be associated with lower energy barriers than the wild type for the (−)-cocaine rotation from the non-prereactive complex to the prereactive complex. Further, (−)-cocaine binding with A328W/Y332G BChE is very similar to the binding with A328W/Y332A BChE, but the position change of F329 residue caused by the (−)-cocaine rotation was significant only in A328W/Y332A BChE, thus suggesting that the energy barrier for the (−)-cocaine rotation in A328W/Y332G BChE should be slightly lower than that in A328W/Y332A BChE.

Table 1 The time-averaged values of some key geometric parameters (Å and degree) in the simulated non-prereactive and prereactive BChE–cocaine complexes [46]

BChE-cocaine binding[a]	Average values of the geometric parameters[c]						RMSD[d]	
	$\langle D1\rangle_{non}$	$\langle D1\rangle$	$\langle D2\rangle$	$\langle D3\rangle$	$\langle D4\rangle$	$\langle\Theta\rangle$	nonpre	pre
Wild type	5.60	3.27	5.77	2.71	3.37	67	1.14	1.27
Wild type with (+)-cocaine[b]	7.64	3.69	2.88	2.30	2.83	61	1.15	1.13
A328W/Y332A	7.11	3.87	3.30	2.14	3.01	51	1.58	1.65
A328W/Y332G	7.06	3.96	2.28	2.52	2.42	60	1.20	1.35
A328W/Y332A/Y419S	5.18	5.84	5.64	4.56	6.97	164	2.66	2.62

[a] Refers to (−)-cocaine binding with wild-type human BChE or (−)-cocaine binding with a mutant BChE, unless indicated otherwise

[b] Refers to (+)-cocaine binding with wild-type human BChE

[c] $\langle D1\rangle_{non}$ and $\langle D1\rangle$ represent the average distances between the S198 O^{γ} atom and the carbonyl carbon of the cocaine benzoyl ester in the simulated non-prereactive and prereactive BChE-cocaine complexes, respectively. $\langle D2\rangle$, $\langle D3\rangle$, $\langle D4\rangle$ refer to the average values of the simulated distances from the carbonyl oxygen of the cocaine benzoyl ester to the NH hydrogen atoms of G116, G117, and A199 residues, respectively. $\langle\Theta\rangle$ is the average value of the dihedral angle formed by the S198 O^{γ} atom and the plane of the carboxylate group of the cocaine benzoyl ester

[d] The root-mean-square deviation (RMSD) of the coordinates of backbone atoms in the simulated structure from those in the X-ray crystal structure of BChE. "nonpre" and "pre" refer to the non-prereactive and prereactive BChE-cocaine complexes, respectively

Concerning (−)-cocaine binding with A328W/Y332A/Y419S BChE, Y419 stays deep inside the protein and does not directly contact with the cocaine molecule [46]. The Y419S mutation was considered because this mutation was initially expected to further increase the free space of the active site pocket so that the (−)-cocaine rotation could be easier. However, as seen in Table 1, the average distance between the carbonyl carbon of cocaine benzoyl ester and S198 O^{γ} atom in the simulated prereactive complex was as long as 5.84 Å. The average distances between the carbonyl oxygen of the cocaine benzoyl ester and the NH hydrolysis atoms of G116, G117, and A199 residues are between 4.56 and 6.97 Å; no any hydrogen bond between them. In addition to the internuclear distances, another interesting geometric parameter is the dihedral angle, Θ, formed by S198 O^{γ} and the plane of the carboxylate group of the cocaine benzoyl ester. As seen in Table 1, the Θ values in the prereactive complexes of cocaine with wild-type BChE and all of the BChE mutants other than A328W/Y332A/Y419S BChE all slightly deviate from the ideal value of 90° for the nucleophilic attack of S198 O^{γ} at the carbonyl carbon of cocaine. The Θ value in the prereactive complex of (−)-cocaine with A328W/Y332A/Y419S BChE is 164°, which is considerably different from the ideal value of 90°.

The above discussion suggests that the energy barriers for the (−)-cocaine rotation in A328W/Y332A and A328W/Y332G BChE's from the non-prereactive complex to the prereactive complex, the rate-determining step for the BChE-catalyzed hydrolysis of (−)-cocaine, should be lower than that in wild-type BChE. Thus, the MD simulations predict that both A328W/Y332A and A328W/Y332G BChE's should have a higher catalytic efficiency than wild-type BChE for (−)-cocaine hydrolysis. Further, the MD simulations also suggest that the energy barrier for the (−)-cocaine rotation in A328W/Y332G BChE should be slightly lower than that in A328W/Y332A BChE and, therefore, the catalytic efficiency of A328W/Y332G BChE for the (-)-cocaine hydrolysis should be slightly higher than that of A328W/Y332A BChE. In addition, the MD simulations predict that A328W/Y332A/Y419S BChE should have no catalytic activity, or have a considerably lower catalytic efficiency than the wild type, for (−)-cocaine hydrolysis because (−)-cocaine binds with the mutant BChE in a way that is not suitable for the catalysis [46]. Following the computational predictions, the wet experimental studies (including site-directed mutagenesis, protein expression, and enzyme activity assay against (−)-cocaine) were carried out [46]. The experimental kinetic data qualitatively confirm the theoretical predictions based on the MD simulations. In particular, the catalytic efficiency of A328W/Y332G BChE is indeed slightly higher than that of A328W/Y332A BChE against (−)-cocaine, and A328W/Y332A/Y419S BChE is indeed inactive against (-)-cocaine [46].

Design of BChE mutants based on transition state simulations

As discussed above, extensive computational modeling and experimental data indicate that (−)-cocaine rotation from the non-prereactive BChE–(−)-cocaine complex to the prereactive BChE–(−)-cocaine complex (ES) is the rate-determining step of (−)-cocaine hydrolysis catalyzed by wild-type BChE [32, 38, 46–49]. Based on the above mechanistic understanding, the earlier efforts for rational design of the BChE mutants were focused on how to improve the ES formation process [38, 46–49]. However, further computational studies and analysis of the experimental data suggest that the rate-determining reaction step for (−)-cocaine hydrolysis catalyzed by the A328W/Y332A and A328W/Y332G mutants becomes the first step of the chemical reaction process, as the hindering of the (−)-cocaine rotation from the non-prereactive BChE–(−)-cocaine complex to the prereactive BChE–(−)-cocaine complex has been removed by the Y332A or Y332G mutation [46, 51, 52]. Therefore, starting from the A328W/Y332A or A328W/Y332G mutant, the rational design of further mutation(s) to improve the catalytic efficiency of BChE against (−)-cocaine can aim to decrease the energy barrier for the first reaction step without significantly affecting the ES formation and other chemical reaction steps [51].

For rational design of high-activity mutants of BChE, a unique computational strategy [51] has been developed to virtually screen various possible BChE mutants based on MD simulations of the rate-determining transition state (i.e., TS1). The unique computational strategy [51] makes possible the MD simulation using a classical force field on a transition state structure. In the design of a high-activity mutant of BChE against (−)-cocaine, one would like to predict some possible mutations that can lower the energy of the transition state for the first chemical reaction step (TS1) and, therefore, lower the energy barrier for this critical reaction step. Apparently, a mutant associated with the stronger hydrogen bonding between the carbonyl oxygen of (−)-cocaine benzoyl ester and the oxyanion hole of the BChE mutant in the TS1 structure may potentially have a more stable TS1 structure and, therefore, a higher catalytic efficiency for (−)-cocaine hydrolysis. Hence, the hydrogen bonding with the oxyanion hole in the TS1 structure is a crucial factor affecting the transition state stabilization and the catalytic activity. The possible effects of some mutations on the hydrogen bonding were examined by performing MD simulations on the TS1 structures

for (−)-cocaine hydrolysis catalyzed by wild-type BChE and its various mutants [51, 52]. The MD simulation in water was performed for 1 ns or longer to make sure that a stable MD trajectory was obtained for each simulated TS1 structure with wild type or mutant BChE. The H···O distances in the simulated TS1 structures for wild-type BChE and its three mutants are summarized in Table 2. The H···O distances between the carbonyl oxygen of (−)-cocaine and the peptidic NH hydrogen atoms of G116, G117, and A199 (or S199) of BChE are denoted by D1, D2, and D3, respectively, in Table 2. D4 in Table 2 refers to the H···O distance between the carbonyl oxygen of (−)-cocaine and the hydroxyl hydrogen of S199 side chain in the simulated TS1 structure corresponding to the A199S/S287G/A328W/Y332G mutant. As seen in Table 2, the simulated H···O distance D1 is always too long for the peptidic NH of G116 to form a N–H···O hydrogen bond with the carbonyl oxygen of (−)-cocaine in all of the simulated TS1 structures. In the simulated TS1 structure for wild-type BChE, the carbonyl oxygen of (−)-cocaine formed a firm N–H···O hydrogen bond with the peptidic NH hydrogen atom of A199 residue; the simulated H···O distance (D3) was 1.61–2.35 Å, with an average D3 value of 1.92 Å. Meanwhile, the carbonyl oxygen of (−)-cocaine also had a partial N–H···O hydrogen bond with the peptidic NH hydrogen atom of G117 residue; the simulated H···O distance (D2) was 1.97–4.14 Å (the average D2 value: 2.91 Å). The average D2 and D3 values became 2.35 and 1.95 Å, respectively, in the simulated TS1 structure for the A328W/Y332A mutant. These distances suggest a slightly weaker N–H···O hydrogen bond with A199, but a stronger N–H···O hydrogen bond with G117, in the simulated TS1 structure for the A328W/Y332A mutant that the corresponding N–H···O hydrogen bonds for the wild type. The average D2 and D3 values (2.25 and 1.97 Å, respectively) in the simulated TS1 structure for the A328W/Y332G mutant are close to the corresponding distances for the A328W/Y332A mutant. The overall strength of the hydrogen bonding between the carbonyl oxygen of (−)-cocaine and the oxyanion hole of the enzyme is not expected to change considerably when wild-type BChE is replaced by the A328W/Y332A or A328W/Y332G mutant.

Table 2 Summary of the MD-simulated key distances (in Å) and the calculated total hydrogen-bonding energies (HBE, in kcal/mol) between the oxyanion hole and the carbonyl oxygen of (−)-cocaine benzoyl ester in the first transition state (TS1) [51, 52]

Transition state	Distance[a]					Total HBE[b]
		D1	D2	D3	D4	
TS1 structure for (−)-cocaine hydrolysis catalyzed by wild-type BChE	Average	4.59	2.91	1.92		−5.5 (−4.6)
	Maximum	5.73	4.14	2.35		
	Minimum	3.35	1.97	1.61		
	Fluctuation	0.35	0.35	0.12		
TS1 structure for (−)-cocaine hydrolysis catalyzed by A328W/Y332A mutant of BChE	Average	3.62	2.35	1.95		−6.2 (−4.9)
	Maximum	4.35	3.37	3.02		
	Minimum	2.92	1.78	1.61		
	Fluctuation	0.23	0.27	0.17		
TS1 structure for (−)-cocaine hydrolysis catalyzed by A328W/Y332G mutant of BChE	Average	3.60	2.25	1.97		−6.4 (−5.0)
	Maximum	4.24	3.17	2.76		
	Minimum	2.89	1.77	1.62		
	Fluctuation	0.23	0.24	0.17		
TS1 structure for (−)-cocaine hydrolysis catalyzed by A199S/F227A/A328W/Y332G mutant of BChE	Average	5.18	2.22	1.96	2.11	−9.8 (−7.4)
	Maximum	5.94	3.08	2.44	3.30	
	Minimum	4.28	1.68	1.65	1.56	
	Fluctuation	0.23	0.21	0.13	0.28	
TS1 structure for (−)-cocaine hydrolysis catalyzed by A199S/S287G/A328W/Y332G mutant of BChE	Average	4.39	2.60	2.01	1.76	−14.0 (−12.0)
	Maximum	5.72	4.42	2.68	2.50	
	Minimum	2.87	1.76	1.62	1.48	
	Fluctuation	0.48	0.36	0.17	0.12	

[a] D1, D2, and D3 represent the internuclear distances between the carbonyl oxygen of cocaine benzoyl ester and the NH hydrogen of residues #116 (i.e., G116), #117 (i.e., G117), and #199 (i.e., A199 or S199) of BChE, respectively. D4 is the internuclear distance between the carbonyl oxygen of cocaine benzoyl ester and the hydroxyl hydrogen of S199 side chain in the A199S/S287G/A328W/Y332G mutant

[b] The total HBE value is the average of the HBE values calculated by using the instantaneous distances in all of the snapshots. The value in parenthesis is the total HBE value calculated by using the MD-simulated average distances

However, the story for the simulated TS1 structures for (−)-cocaine catalyzed by the A199S/F227A/A328W/Y332G and A199S/S287G/A328W/Y332G mutants were remarkably different. As one can see from Table 2, when residue #199 becomes a serine (i.e., S199), the hydroxyl group on the side chain of S199 can also hydrogen bond to the carbonyl oxygen of (−)-cocaine to form an O–H···O hydrogen bond, in addition to the two N–H···O hydrogen bonds with the peptidic NH of G117 and S199. For the A199S/F227A/A328W/Y332G mutant, the simulated average H···O distances with the peptidic NH hydrogen of G117, peptidic NH hydrogen of S199, and hydroxyl hydrogen of S199 are 2.22, 1.96, and 2.11 Å, respectively. For the A199S/S287G/A328W/Y332G mutant, the simulated average H···O distances with the peptidic NH hydrogen of G117, peptidic NH hydrogen of S199, and hydroxyl hydrogen of S199 are 2.60, 2.01, and 1.76 Å, respectively. Due to the additional O–H···O hydrogen bond, the overall strength of the hydrogen bonding with the modified oxyanion hole of A199S/F227A/A328W/Y332G or A199S/S287G/A328W/Y332G BChE should be significantly stronger than that of wild type, A328W/Y332A and A328W/Y332G BChE's.

To better represent the overall strength of hydrogen bonding between the carbonyl oxygen of (−)-cocaine and the oxyanion hole in a MD-simulated TS1 structure, the hydrogen bonding energy (HBE) associated with each simulated H···O distance was estimated [51, 52] by using a HBE equation implemented in AutoDock 3.0 program suite [53]. For each hydrogen bond with the carbonyl oxygen of (−)-cocaine, a HBE value can be evaluated with each snapshot of the MD-simulated structure. The final HBE of the MD-simulated hydrogen bond is considered to be the average HBE value of all snapshots taken from the stable MD trajectory. The estimated total HBE value for the hydrogen bonds between the carbonyl oxygen of (−)-cocaine and the oxyanion hole in each simulated TS1 structure is also shown in Table 2.

The HBE for each hydrogen bond was also estimated by using the MD-simulated average H···O distance. As seen in Table 2, the total hydrogen-bonding energies (i.e., −4.6, −4.9, −5.0, −7.4, and −12.0 kcal/mol for the wild type, A328W/Y332A, A328W/Y332G, A199S/F227A/A328W/Y332G, and A199S/S287G/A328W/Y332G BChE's, respectively) estimated in this way are systematically higher (i.e., less negative) than the corresponding total hydrogen-bonding energies (i.e., −5.5, −6.2, −6.4, −9.8, and −14.0 kcal/mol) estimated in the aforementioned way. However, the two sets of total HBE values are qualitatively consistent with each other in terms of the relative hydrogen-bonding strengths in the four simulated TS1 structures. In particular, the two sets of total HBE values consistently reveal that the overall strengths of the hydrogen bonding between the carbonyl oxygen of (−)-cocaine and the oxyanion hole in the simulated TS1 structure for A199S/F227A/A328W/Y332G and A199S/S287G/A328W/Y332G BChE's [51, 52] are significantly stronger than that for wild type, A328W/Y332A, and A328W/Y332G BChE's.

The computational results discussed above suggest that the transition states for the first chemical reaction step (TS1) of (−)-cocaine hydrolysis catalyzed by the A199S/F227A/A328W/Y332G and A199S/S287G/A328W/Y332G mutants should be significantly more stable than that by the A328W/Y332A or A328W/Y332G mutant, due to the significant increase of the overall hydrogen bonding between the carbonyl oxygen of (−)-cocaine and the oxyanion hole of the enzyme in the TS1 structure. Further, the TS1 structure associated with the A199S/S287G/A328W/Y332G mutant should be more stable than that associated with the A199S/F227A/A328W/Y332G mutant. The aforementioned analysis of the literature also indicates that the first chemical reaction step associated with TS1 should be the rate-determining step of (−)-cocaine hydrolysis catalyzed by a BChE mutant including Y332A or Y332G mutation, although the formation of the prereactive enzyme-substrate complex (ES) is the rate-determining step for (−)-cocaine hydrolysis catalyzed by wild-type BChE. This suggests a clear correlation between the TS1 stabilization and the catalytic efficiency of A328W/Y332A, A328W/Y332G, A199S/F227A/A328W/Y332G, and A199S/S287G/A328W/Y332G BChE's for (−)-cocaine hydrolysis: the more stable the TS1 structure, the lower the energy barrier, and the higher the catalytic efficiency. Thus, the MD simulations predict that both A199S/F227A/A328W/Y332G and A199S/S287G/A328W/Y332G BChE's should have a higher catalytic efficiency than A328W/Y332A or A328W/Y332G BChE for (−)-cocaine hydrolysis. Further, the A199S/S287G/A328W/Y332G mutant is expected to be more active than the A199S/F227A/A328W/Y332G mutant.

The computational predictions based on the transition state simulations were followed by wet experiments [51, 52]. The wet experiments revealed that A199S/S287G/A328W/Y332G BChE has a ∼456-fold improved catalytic efficiency against (−)-cocaine compared to the wild type, or A199S/S287G/A328W/Y332G BChE has a k_{cat}/K_M value of $\sim 4.15 \times 10^8$ M min^{-1} for (−)-cocaine hydrolysis [51]. It was also determined that A199S/F227A/A328W/Y332G BChE has a ∼151-fold improved catalytic efficiency against (−)-cocaine compared to the wild type, or A199S/F227A/A328W/Y332G BChE has a k_{cat}/K_M value of $\sim 1.37 \times 10^8$ M min^{-1} against (−)-cocaine [52]. By using the designed A199S/S287G/A328W/Y332G BChE as an exogenous enzyme in human, when the concentration of this mutant is kept the same as that of the wild-type BChE in plasma, the half-life time of

(−)-cocaine in plasma should be reduced from the ~45–90 min to only ~6–12 s, considerably shorter than the time required for cocaine crossing the blood-brain barrier to reach CNS [51]. Hence, the encouraging outcome of the rational design and discovery study could eventually result in a valuable, efficient anti-cocaine medication.

Concluding remarks

An extensive summary of the computational design of high-activity mutants of human butyrylcholinesterase (BChE) against (−)-cocaine (the abused cocaine) has been presented. The computational design of BChE mutants has been based on not only the structure of the enzyme, but also the detailed catalytic mechanisms for BChE-catalyzed hydrolysis of (−)-cocaine and (+)-cocaine. Computational studies of the detailed catalytic mechanisms and the structure- and mechanism-based computational design have been carried out through the combined use of a variety of state-of-the-art techniques of molecular modeling. The used computational techniques include the homology modeling, molecular docking, molecular dynamics simulations, first-principles electronic structure calculations, and hybrid quantum mechanical/molecular mechanical calculations. These state-of-the-art computational studies have led to detailed mechanistic insights into the reaction pathways for BChE-catalyzed hydrolysis of (−)-cocaine and (+)-cocaine. These detailed mechanistic insights provide a solid basis for rational design of novel anti-cocaine medication using the high-activity mutants of human BChE.

By using the computational insights into the catalytic mechanisms for BChE-catalyzed hydrolysis of (−)-cocaine and (+)-cocaine, two types of computational design methods/strategies have been employed to design and discover the high-activity mutants of human BChE. The first design method is based on modeling and simulation of the enzyme-substrate binding that aim to improve the formation of prereactive BChE-(−)-cocaine binding, when the formation of prereactive BChE-(−)-cocaine binding is a rate-determining step. When the rate-determining step becomes the chemical reaction process, the truly rational design of the BChE mutants cannot be limited to the simulation of the enzyme-substrate binding. A unique computational design strategy based on the simulation of the rate-determining transition state has been developed to design high-activity mutants of human BChE for hydrolysis of (−)-cocaine, leading to the exciting discovery of BChE mutants with a considerably improved catalytic efficiency against (−)-cocaine. One of the discovered BChE mutants (i.e., A199S/S287G/A328W/Y332G) has a ~456-fold improved catalytic efficiency against (−)-cocaine. The encouraging outcome of the computational design and discovery effort demonstrates that the unique computational design approach based on the transition-state simulation is promising for rational enzyme redesign and drug discovery.

The similar computational strategy in combination with appropriate wet experiments may also be useful in rational redesign of many other metabolic enzymes for the therapeutic treatments of metabolic diseases.

Acknowledgment Financial support from the National Institute on Drug Abuse (NIDA) of National Institutes of Health (NIH) (grant R01 DA013930) and extensive supercomputing time support from University of Kentucky Center of Computational Sciences are gratefully acknowledged.

References

1. Gawin FH, Ellinwood EHN Jr (1998) Eng J Med 318:1173
2. Landry DW (1997) Scientific American 276:28
3. Singh S (2000) Chem Rev 100:925
4. Sparenborg S, Vocci F, Zukin S (1997) Drug Alcohol Depend 48:149
5. Gorelick DA (1997) Drug Alcohol Depend 48:159
6. Gorelick DA, Gardner EL, Xi Z-X (2004) Drugs 64:1547–1573
7. Baird TJ, Deng S-X, Landry DW, Winger G, Woods JH (2000) J Pharmacol Exp Ther 295:1127–1134
8. Carrera MRA, Ashley JA, Wirsching P, Koob GF, Janda KD (2001) Proc Natl Acad Sci USA 98:1988–1992
9. Deng S-X, de Prada P, Landry DW (2002) J Immunol Methods 269:299–310
10. Kantak KM (2003) Expert Opin Pharmacother 4:213–218
11. Carrera MRA, Kaufmann GF, Mee JM, Meijler MM, Koob GF, Janda KD (2004) Proc Natl Acad Sci USA 101:10416–10421
12. Dickerson TJ, Kaufmann GF, Janda KD (2005) Expert Opin Biol Therapy 5:773–781
13. Meijler MM, Kaufmann GF, Qi LW, Mee JM, Coyle AR, Moss JA, Wirsching P, Matsushita M, Janda KD (2005) J Am Chem Soc 127:2477–2484
14. Rogers CJ, Mee JM, Kaufmann GF, Dickerson TJ, Janda KD (2005) J Am Chem Soc 127:10016–10017
15. Carrera MRA, Ashley JA, Parsons LH, Wirsching P, Koob GF, Janda KD (1995) Nature 378:727–730
16. Fox BS (1997) Drug Alcohol Depend 100:153–158
17. Carrera MRA, Ashley JA, Zhou B, Wirsching P, Koob GF, Janda KD (2000) Proc Natl Acad Sci USA 97:6202–6206
18. Carrera MRA, Ashley JA, Wirsching P, Koob GF, Janda KD (2001) Proc Natl Acad Sci USA 98:1988–1992
19. Carrera MRA, Trigo JM, Roberts AJ, Janda KD (2005) Pharmacol Biochem Behav 81:709–714
20. Fox BS, Kantak KM, Edwards MA, Black KM, Bollinger BK, Botka AJ, French TL, Thompson TL, Schad VC, Greenstein JL, Gefter ML, Exley MA, Swain PA, Briner TJ (1996) Nat Med 2:1129–1132
21. Kantak KM, Collins SL, Bond J, Fox BS (2001) Psychopharmacology 153:334–340
22. Landry DW, Yang GX-Q (1997) J Addict Diseases 16:1–17
23. Landry DW, Zhao K, Yang GX-Q, Glickman M, Georgiadis TM (1993) Science 259:1899–1901
24. Matsushita M, Hoffman TZ, Ashley JA, Zhou B, Wirsching P, Janda KD (2001) Bioorg Med Chem Lett 11:87–90

25. Cashman JR, Berkman CE, Underiner GE (2000) J Pharm Exp Ther 293:952–961
26. Yang G, Chun J, Arakawa-Uramoto H, Wang X, Gawinowicz MA, Zhao K, Landry DW (1996) J Am Chem Soc 118: 5881–5890
27. Gately SJ (1991) Biochem Pharmacol 41:1249–1254
28. Gately SJ, MacGregor RR, Fowler JS, Wolf AP, Dewey SL, Schlyer DJ (1990) J Neurochem 54:720–723
29. Darvesh S, Hopkins DA, Geula C (2003) Nature Rev Neurosci 4:131–138
30. Giacobini E (ed) (2003) Butyrylcholinesterase: its function and inhibitors. Dunitz Martin Ltd, Great Britain
31. Keating GM, Simpson D (2007) Drugs 67:435–455
32. Zhan C-G, Zheng F, Landry DW (2003) J Am Chem Soc 125:2462–2474
33. Masson P, Legrand P, Bartels CF, Froment M-T, Schopfer LM, Lockridge O (1997) Biochemistry 36:2266
34. Li P, Zhao K, Deng S, Landry DW (1999) Helvetica Chim Acta 82:85
35. Zhan C-G, Landry DW (2001) J Phys Chem A 105:1296
36. Harel M, Sussman JL, Krejci E, Bon S, Chanal P, Massoulie J, Silman I (1992) Proc Natl Acad Sci USA 89:10827
37. Masson P, Xie W, Froment M-T, Levitsky V, Fortier P-L, Albaret C, Lockridge O (1999) Biochim Biophys Acta 1433:281
38. Sun H, Yazal JE, Lockridge O, Schopfer LM, Brimijoin S, Pang YP (2001) J Biol Chem 276:9330–9336
39. Hu C-H, Brinck T, Hult K (1998) Int J Quantum Chem 69:89
40. Wlodek ST, Clark TW, Scott L, McCammon JAJ (1997) Am Chem Soc 119:9513
41. Wlodek ST, Antosiewicz J, Briggs JM (1997) J Am Chem Soc 119:8159
42. Zhou H-X, Wlodek ST, McCammon JA (1998) Proc Natl Acad Sci USA 95:9280
43. Malany S, Sawai M, Sikorski RS, Seravalli J, Quinn DM, Radic Z, Taylor P, Kronman C, Velan B, Shafferman A (2000) J Am Chem Soc 122:2981
44. Gao D, Zhan C-G (2005) J Phys Chem B 109:23070–23076
45. Zhan C-G, Gao D (2005) Biophysical Journal 89:3863
46. Hamza A, Cho H, Tai H-H, Zhan C-G (2005) J Phys Chem B 109:4776
47. Gao D, Zhan C-G (2006) Proteins 62:99–110
48. Sun H, Shen ML, Pang YP, Lockridge O, Brimijoin S (2002) J Pharmacol Exp Ther 302:710–716
49. Sun H, Pang YP, Lockridge O, Brimijoin S (2002) Mol Pharmacol 62:220–224
50. Gao Y, Atanasova E, Sui N, Pancook JD, Watkins JD, Brimijoin S (2005) Mol Pharmacol 67:204–211
51. Pan Y, Gao D, Yang W, Cho H, Yang G-F, Tai H-H, Zhan C-G (2005) Proc Natl Acad Sci USA 102:16656
52. Gao D, Cho H, Yang W, Pan Y, Yang G-F, Tai H-H, Zhan C-G (2006) Angew Chem Int Ed 45:653–657
53. Morris GM, Goodsell DS, Halliday RS, Huey R, Hart WE, Belew RK, Olson AJJ (1998) Comput Chem 19:1639